Journal of *Marine Science and Engineering*

MDPI

Article

A New Method of Ship Type Identification Based on Underwater Radiated Noise Signals

Shanshan Chen [1,2], Sheng Guan [2,3,4,5,*], Hui Wang [2,3,4,5], Ningqi Ye [2,3,4,5] and Zexun Wei [2,3,4,5]

[1] College of Underwater Acoustic Engineering, Harbin Engineering University, Harbin 150001, China; 13295387515@163.com
[2] First Institute of Oceanography, Ministry of Natural Resources, Qingdao 266061, China
[3] Key Laboratory of Marine Science and Numerical Modeling, First Institute of Oceanography, Ministry of Natural Resources, Qingdao 266061, China
[4] Laboratory for Regional Oceanography and Numerical Modeling, Pilot National Laboratory for Marine Science and Technology, Qingdao 266061, China
[5] Shandong Key Laboratory of Marine Science and Numerical Modeling, Qingdao 266061, China
* Correspondence: gsh30@163.com

Abstract: Ship type identification is an important basis for ship management and monitoring. The paper proposed a new method of ship type identification by combining characteristic parameters from the energy difference between high and low frequencies and the sensitive IMF variance mean value based on the modal decomposition of the underwater radiated noise signals using the Ensemble Empirical Mode Decomposition (EEMD) method. The comparison shows that the characteristic parameters of different types of ship, underwater radiated noises are different, whereas those of the same types of ship, underwater radiated noises fall in close range. Validation experiments based on randomly selected ship underwater radiated noise samples manifest that the method is of good separability for the four types of ship underwater radiated noises in the Deepship dataset. It has a higher identification rate than other methods within the distance range of ship underwater radiated noise detection in the dataset. The accuracy of this method tends to decrease with distance in the classification experiments of the ship underwater radiated noises at different distances.

Keywords: signals processing; ship underwater radiated noise; ship type identification; ensemble empirical mode decomposition

Citation: Chen, S.; Guan, S.; Wang, H.; Ye, N.; Wei, Z. A New Method of Ship Type Identification Based on Underwater Radiated Noise Signals. *J. Mar. Sci. Eng.* **2023**, *11*, 963. https://doi.org/10.3390/jmse11050963

Academic Editor: Nikolaos I. Xiros

Received: 18 April 2023
Revised: 25 April 2023
Accepted: 27 April 2023
Published: 30 April 2023

1. Introduction

Ships play an important role as a major tool for marine development and exploration. Ships inevitably emit a range of radiated noises when navigating at sea. The monitoring and analysis of ship noise allow for effective monitoring and management of ships, which can promote the development of the maritime industry and ensure maritime safety with great security and military significance [1–3]. The noise can be divided into two main parts: airborne ship noise and underwater radiation noise.

Airborne noise can be detrimental to the health of navigators and people living in the vicinity of ports; people are more conscious of the safety of their living environment and are more concerned and protesting about the dangers of airborne noise [4,5], so there is a need to monitor the airborne noise generated by ships in operation. By studying the type of vessel, it is possible to map the noise generated by the movement of the vessel and avoid noise complaints; by calculating the sound power level and power spectrum when the vessel is sailing at low speed, it is possible to measure the continuous noise of the vessel and correctly estimate the noise impact [6]; through acoustic measurements, it is possible to understand the correlation between parameters such as minimum distance, speed, and draft and the noise emissions from the vessel [7]; for the prevention and management of noise in ports, the development of a number of procedures and databases [8–10] allows for

a refined classification of port noise sources and the identification of responsible sources from control.

Underwater radiated noise, as another component of ship radiated noise, is more significant in scientific research, and all the ship radiated noise in this paper refers to underwater radiated noise. The noise generated by a ship during operation contains many ship characteristics [11,12], such as propeller speed, mechanical vibration, sailing speed, tonnage, ship type, etc. Therefore, the classification and identification of ship types can be accomplished by extracting ship radiation noise features. Because ships (especially civilian ships) carry a large amount of cargo, traffic management and safety monitoring of ports can be used to achieve traffic prediction and improve port operation models.

Traditional methods for extracting the features of ship radiation noise mainly include Fourier Transform (FT), Short-time Fourier Transform (STFT), and Wavelet Transform (WT), but these methods all have some problems. FT can clearly obtain the frequency spectrum of the signal but cannot determine the frequency component of a certain time period [13,14]; STFT adds a window function to achieve time-frequency analysis, but the shape does not change after the window function is determined, and the resolution is determined, and the time and frequency resolution cannot be optimal at the same time [15,16]; WT can observe both frequency and time axes, with good temporal resolution at high frequencies and good frequency resolution at low frequencies [17–22], but WT requires the selection of a suitable wavelet basis, and this selection is challenging. Empirical Mode Decomposition (EMD) can decompose the original signal into a finite number of Intrinsic Mode Functions (IMFs) by adaptively decomposing the signal according to its own scale characteristics, and EMD has a more difficult choice of instantaneous EMD describes the instantaneous frequency, so it is easier to decompose nonlinear non-smooth signals [23], but this method suffers from endpoint effects and mode mixing problems, so Ensemble Empirical Mode Decomposition (EEMD) is proposed to add Gaussian white noise of equal amplitude to the original signal several times, and the decomposition results are averaged to obtain IMF component [24]. In this paper, the EEMD is used to extract features from the ship's radiation noise.

The features selected for feature extraction of the ship's radiated noise are stable and are mainly based on frequency, energy, and entropy. One direction is to select single features or double features as extraction parameters [25], proposed a single-feature method based on slope entropy (SlEn) and a dual-feature method with SlEn combined with permutation entropy (SlEn and PE) and verified the superiority of the dual-feature extraction method. In [16], a multi-stage feature extraction method combining enhanced variational mode decomposition (EVMD), weighted permutation entropy (WPE), and local tangent space alignment (LTSA) was used to extract hydroacoustic signal features. Another direction is to propose a combination of decomposition methods and feature extraction methods. In [26], based on variational mode decomposition (VMD), the fluctuation-based dispersion entropy (FDE) of each IMF is differenced from the original signal, and the IMF corresponding to the minimum value is filtered out and its FDE is used as the feature value for classification. The method has a good separation effect. In [27], the Slope entropy (Slopen) was studied on the basis of complete ensemble empirical mode decomposition with adaptive noise (CEEMDAN), and a feature extraction method with dual IMF optimization was proposed. In this paper, a dual feature parameter extraction method based on the cumulative mean principle (MSAM) for high and low frequency energy difference and sensitive IMF variance mean is proposed based on EEMD. The remaining structure is as follows: Section 2 introduces the source of the dataset and the data processing method; Section 3 presents the classification method and the results; Section 4 discusses and extends the applicability of the method and concludes with the conclusion.

2. Data and Method

2.1. Source and Pre-Processing of Ship Underwater Radiated Noise Data

In this paper, the feature extraction of ship underwater radiated noise signals is based on the DeepShip dataset [28]. The dataset collects real underwater radiated noise from

265 ships entering and leaving Vancouver Harbor, with ship types including tugs, cargos, passenger ships, and tankers. The sampling period is from 2 May 2016 to 4 October 2018, with a total duration of 47 h 4 min. Each underwater radiated noise sample is a 2 km radius from the location of the hydrophone location when only one ship is present, and that ship is emitting a navigation underwater radiated noise signal. Data acquisition stops when the vessel moves out of the 2 km range of the hydrophone. The hydrophone bandwidth is 1 Hz~12 kHz, a sensitivity of −170 dBV re.μPa, and a sampling frequency of 32 kHz. The hydrophones are deployed at depths of 141 m, 144 m, and 147 m below sea level.

The original dataset contains a total of 613 records, including 70 tugs, 110 cargos, 193 passenger ships, and 240 tankers. Since the data recording site is located on the busiest shipping lane of the Pacific Northwest coast, and there are marine organisms such as whales and salmon activities, it is necessary to filter the data set to eliminate the suspected natural background noise, marine mammal noise, and other human activity noise, and to select only the sampling of the same ship closest to the hydrophone position; finally, a total of 340 underwater radiated noise signals are obtained, including 84 cargo underwater radiated noise signals, 113 passenger ship underwater radiated noise signals, 110 tanker underwater radiated noise signals and 33 tug underwater radiated noise signals.

The Nyquist sampling theorem states that the sampling frequency must be greater than or equal to twice the highest frequency of the signals, the digital signal's obtained by sampling, in order to preserve the original signals information. Therefore, if the hydrophone sampling frequency is set to 16 kHz, the effective signals frequency of the collected ship underwater radiated noise will be less than 8 kHz.

For the above ship underwater radiated noise signals, firstly, pre-processing is performed. Secondly, the signals are normalized to obtain the time domain waveforms of four types of ship underwater radiated noise, and one representative signal of each type is randomly selected, as shown in the left panel of Figure 1a–d. Time-frequency analysis is performed on the underwater radiated noise, and the results are shown in the middle panel of Figure 1a–d. Time-frequency analysis can clearly describe the relationship between signal frequency and time. It is observed that the main frequency bands of the four types of underwater radiated noise signals are below 1000 Hz, and the main frequency band distribution can be seen in Table 1, and there is no regularity in the fundamental harmonic distribution of different types of underwater radiated noise. Power spectrum analysis of underwater radiated noise results are shown in the right panel of Figure 1a–d, which indicates the variation of underwater radiated noise power with frequency, that is, the distribution of underwater radiated noise power in the frequency domain, observation can be seen from the power spectrum of cargo underwater radiated noise extreme value of 121.5 dB, the power spectrum of passenger ships underwater radiated noise extreme value of 116.9 dB, the power spectrum of tug underwater radiated noise extreme value of 117.7 dB, tanker underwater radiated noise Through the experimental results of the above analysis means, it can be seen that the traditional combined time-frequency domain method cannot effectively classify the ships according to the ship underwater radiated noise.

Table 1. The main frequency ranges of ship underwater radiated noises.

Type	Main Frequency Range/Hz	Type	Main Frequency Range/Hz
Oil tanker underwater radiated noise	9.6~594.2	cargo vessel underwater radiated noise	11.6~649.6
Tugboat underwater radiated noise	35.4~712.2	Passenger ship underwater radiated noise	9.4~882.8

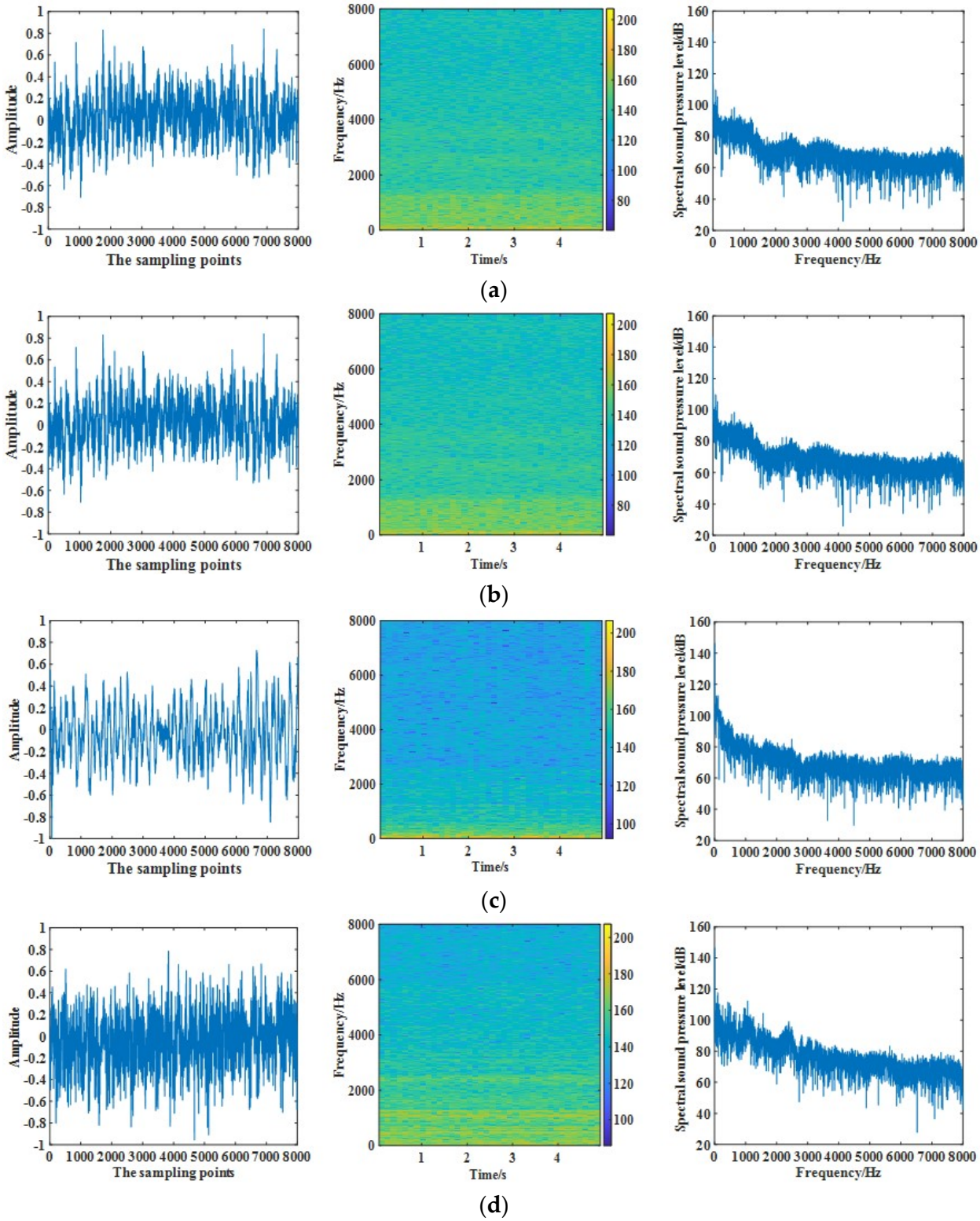

Figure 1. Time-frequency analysis of the ship underwater radiated noise signals. (**a**) Example of time-frequency analysis of cargo underwater radiated noise; (**b**) Example of time-frequency analysis of passenger ships underwater radiated noise; (**c**) Example of time-frequency analysis of tanker underwater radiated noise; (**d**) Example of time-frequency analysis of tug underwater radiated noise.

2.2. Ship Underwater Radiated Noise Data Processing Method

For real signals measured in the field, the data are non-linear and non-stationary, so the traditional feature extraction methods are no longer applicable. In this paper, the EEMD method is used to extract features from ship radiation noise signals.

EEMD is used to change the polar distribution of the signals by adding random white noise of equal amplitude to the original signals several times to homogenize the distribution of the polar points and to avoid the effects of intermittent high frequency components [24]. The eigenmode function (IMF) obtained by EMD is then averaged overall averaged several times to cancel the added white noise, thus preserving the meaningful IMF components.

The specific steps are:

(1) Superimposing N white noise sequences of a given amplitude onto the original data set $X(t)$ to be analyzed to obtain N new sequences $x(t)$.
(2) Perform an empirical modal decomposition on the new signal $x(t)$.
(3) Repeat the above two steps, adding new white noise sequences of the same amplitude each time to obtain different IMFs.
(4) Perform a pooled average of the IMFs obtained from each decomposition so that the added white noise cancels each other out, and use them as the final decomposition results.

$$C_j(t) = \frac{1}{N}\sum_{i=1}^{N} C_{ij}(t) \tag{1}$$

where $C_j(t)$ is the j_{th} IMF component finally obtained, N is the number of white noise sequences, and $C_{ij}(t)$ represents the j_{th} IMF component after adding the i_{th} white noise.

Following the above steps, the EEMD decomposition of multiple ship radiation sounds was performed separately. When selecting the ship underwater radiated noise samples, the data with the same distance between the hydrophone and the ship were selected to improve the comparability of the results and to reduce the influence of hydroacoustic channels. The signal data lengths were sampled at 8000 points, and white noise with 100 times the mean value of zero and a standard deviation of 0.3 times the standard deviation of the signals to be decomposed was added to the underwater radiated noise signals.

The results of the decomposition are shown in Figure 2, where the horizontal coordinate indicates the number of sampling points, and the vertical coordinate indicates the amplitude of the modal components. The analysis shows that: (1) The order of the IMF varies with the complexity of the signals. The more complex the signals are, the more orders of the intrinsic mode function component (IMF) are obtained from the decomposition. (2) After decomposing different types of underwater radiated noise by EEMD, a set of IMFs from high frequency to low frequency is obtained. (3) The first-order intrinsic mode function component IMF1 indicates the shortest oscillation period of oscillation of the signals. (4) After the underwater radiated noise signals have been decomposed by EEMD, the signal energies are concentrated in the first few IMF components, reflecting the most significant and important information in the original signals.

2.3. Algorithm of High and Low Frequency Energy Difference Based on MSAM Principle

In order to select the IMF components with a strong correlation with the ship underwater radiated noise signals, this paper uses the cumulative mean based (MSAM) as a selection criterion to separate the high frequency IMF components from the low frequency IMF components. The MSAM principles are defined as follows:

$$h_v = mean\left[\sum_{i=1}^{v}\left[IMF^i(t)\right] - \frac{mean(IMF^i(t)}{std(IMF^i(t)}\right], v \le N \tag{2}$$

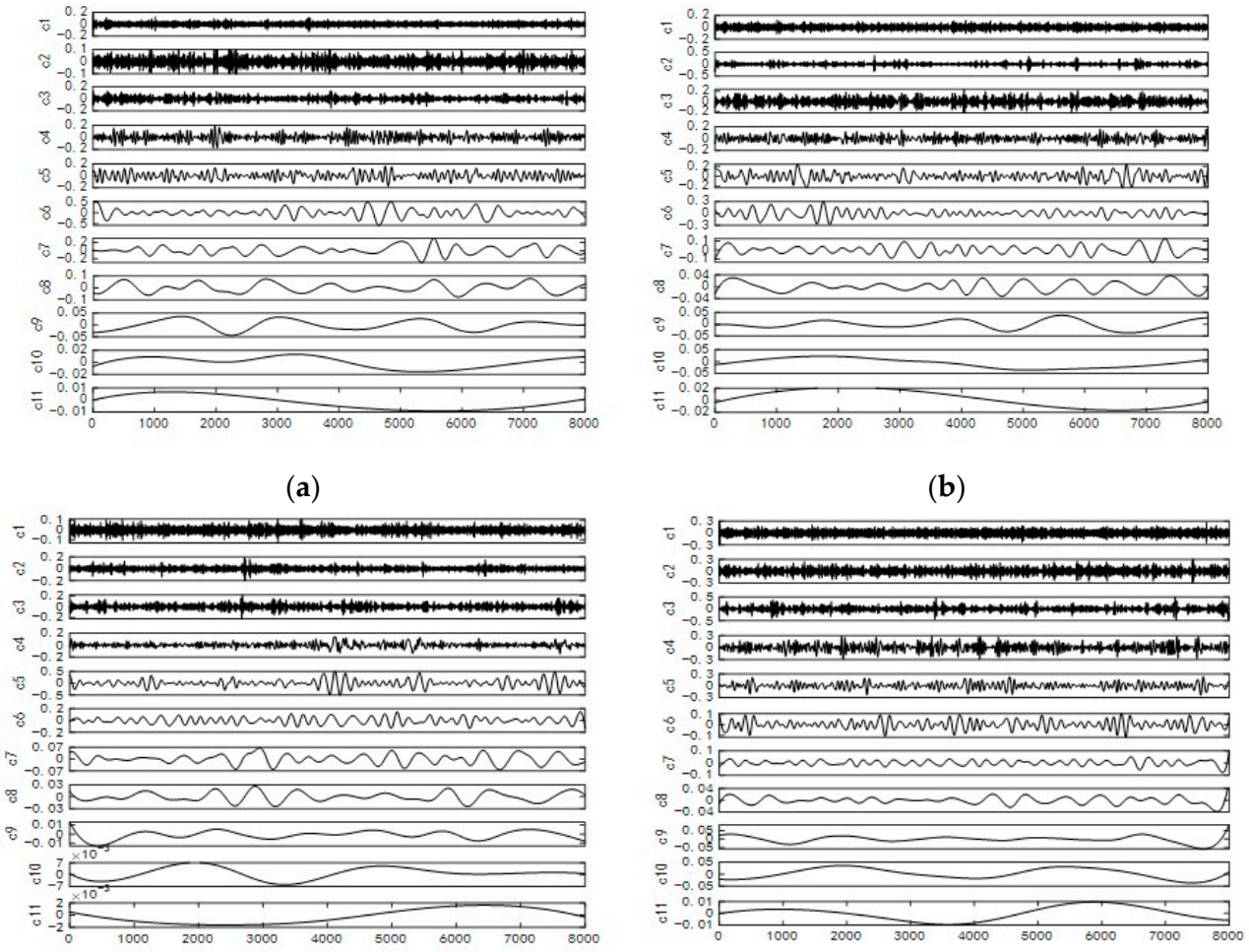

Figure 2. IMF components of ship underwater radiated noises decomposed by EEMD; (**a**) cargo vessel underwater radiated noise; (**b**) passenger ship underwater radiated noise; (**c**) oil tanker underwater radiated noise; (**d**) tugboat underwater radiated noise.

The v where h_v starts to deviate from zero is used as a marker to separate the high frequency *IMF* component from the low frequency *IMF* component. One sample of each type of ship underwater radiated noise is selected as an example, and the *IMF* component of the underwater radiated noise signals is divided into the high frequency *IMF* component region and the low frequency *IMF* component region using the MSAM criterion, and the results are shown in Figure 3. Among them, cargo underwater radiated noise $h_v = -0.0588$, passenger ship underwater radiated noise $h_v = 0.0108$, tanker underwater radiated noise $h_v = -0.0282$, and tug underwater radiated noise $h_v = -0.0428$. According to Equation (2), it can be calculated that the boundary scale of the high and low frequency modal component area of cargo underwater radiated noise is 5, passenger ship underwater radiated noise is 3, tanker underwater radiated noise is 5, and tug underwater radiated noise is 6 (The serial number corresponding to the solid red circle in Figure 3).

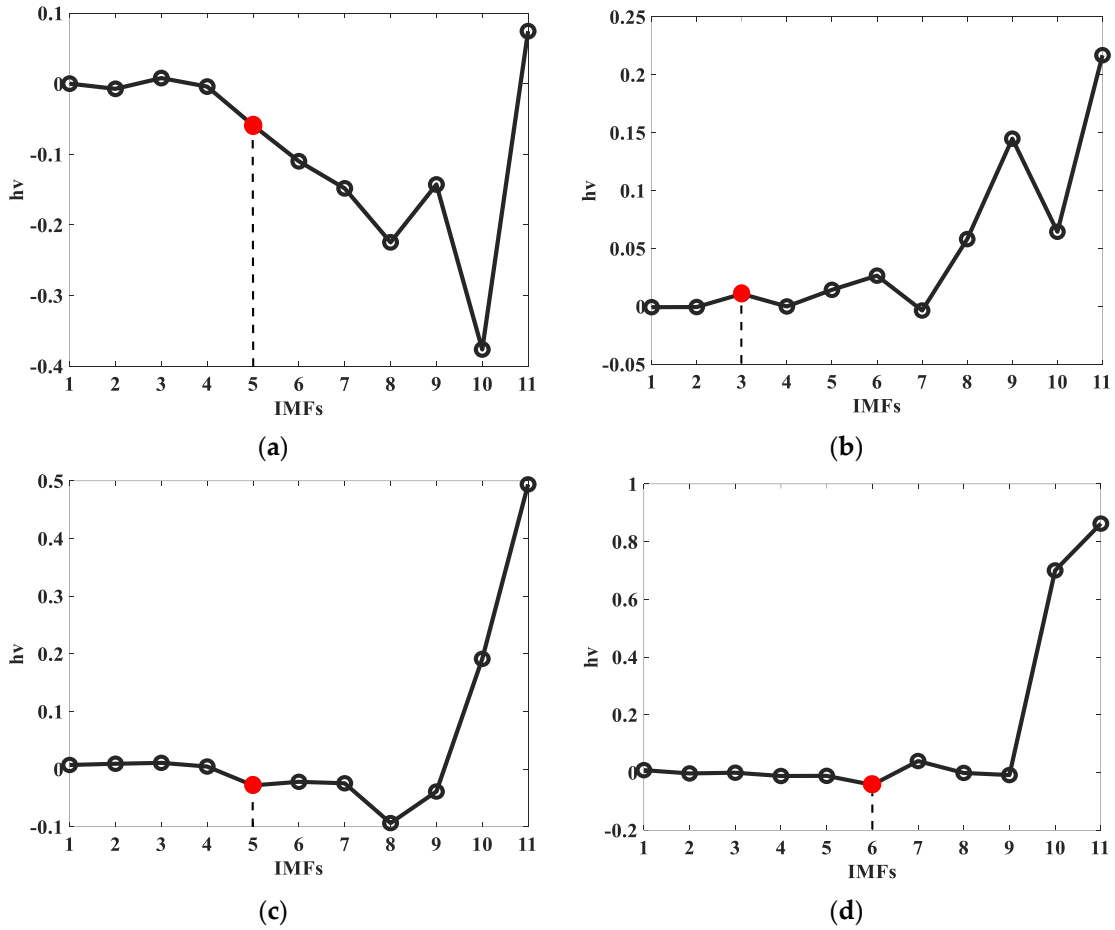

Figure 3. MSAM values of the ship underwater radiated noises (single sample). (**a**) cargo vessel underwater radiated noise; (**b**) passenger ship underwater radiated noise; (**c**) oil tanker underwater radiated noise; (**d**) tugboat underwater radiated noise.

EEMD decomposition of the signal $x(t)$ can be obtained after the IMF component, for which the Hilbert transform can be obtained $H(x)$, for $H(x)$ to find its real and imaginary parts to obtain $\mathrm{Re}(x)$ and $\mathrm{Im}(x)$, the instantaneous amplitude is:

$$A = \sqrt{\mathrm{Re}^2(x) + \mathrm{Im}^2(x)} \tag{3}$$

The instantaneous intensity is:

$$B = A^2 \tag{4}$$

Let the instantaneous intensity of each IMF band sampling point in the high frequency band modal region be $B_{H1}, B_{H2}, B_{H3}, \ldots, B_{Hm}$, then the total energy of the high frequency band is:

$$E_H = 10\lg \sum_{j=v}^{i} \left(\sum_{k=1}^{m} B_{HK} \right) \tag{5}$$

Let the instantaneous intensity of each IMF band sampling point in the low frequency band modal region be $B_{L1}, B_{L2}, B_{L3}, \ldots, B_{Ln}$, then the total energy of the low frequency band is:

$$E_L = 10\lg \sum_{j=v}^{i} \left(\sum_{k=1}^{n} B_{LK} \right) \tag{6}$$

where v is the scale separating the high frequency IMF component from the low frequency IMF component; m and n are the number of sampling points in each IMF frequency band, where $m = n = 8000$; i is the order of the IMF component.

The energy difference between the high and low frequencies of the signals is:

$$E_\Delta = E_H - E_L \tag{7}$$

2.4. Algorithm of Sensitive IMF Mean of Variance

From the sample experimental results, the adaptive high and low frequency energy difference as a characteristic parameter for ship type identification can be separated from other types of ships for tanker underwater radiated noise, but the value distribution varies widely and is confused with other types of ships to some extent. So considered whether the accuracy of type identification can be further improved by increasing the feature parameters.

After the EEMD decomposition of the underwater radiated noise signals, the signals are decomposed into several IMF components in the order from high frequency to low frequency, where one part of the IMF is the sensitive component closely related to the ship underwater radiated noise, and the other part is the irrelevant component and the underwater radiated noise component. Therefore, the sensitive IMF of the ship underwater radiated noise can be selected and the other irrelevant IMF components can be removed to improve the accuracy of the feature extraction. The steps are as follows:

(1) Calculate the correlation coefficient between the signal $x(t)$ and the IMF components. Define the correlation coefficient r:

$$r = \frac{\sum_{i=1}^{n}(x_i - \overline{x})(c_i - \overline{c})}{\sqrt{\sum_{i=1}^{n}(x_i - \overline{x})^2 \bullet \sum_{i=1}^{n}(c_i - \overline{c})^2}} = \frac{n\sum_{i=1}^{n} x_i c_i - \sum_{i=1}^{n} x_i \bullet \sum_{i=1}^{n} c_i}{\sqrt{n\sum_{i=1}^{n} x_i{}^2 - (\sum_{i=1}^{n} x_i)^2} \bullet \sqrt{n\sum_{i=1}^{n} c_i{}^2 - (\sum_{i=1}^{n} c_i)^2}} \tag{8}$$

where $x(t)$ is the original signals, i is the order of the IMF component, and c is the decomposed IMF component.

(2) Calculate the IMF sensitive factor of the signal $x(t)$:

$$\lambda_i = \frac{r_i - \min(r)}{\max(r) - \min(r)} i = 1, 2, \ldots, n \tag{9}$$

where i is the order of the IMF component, n is the number of sampling points.

(3) Select sensitive IMF according to sensitive factors.

Sort all IMFs in descending order of sensitivity. Sensitive factor sequence and IMF sequence can be obtained to calculate the difference between the sensitive factors of two adjacent IMFs:

$$d_i = \lambda_i{}' - \lambda_{i+1}{}' \tag{10}$$

Find the subscript i corresponding to the maximum difference, then the first i IMFs (~) are the sensitive IMFs of the underwater radiated noise signals.

(4) The variance of the sensitive IMF can be calculated as follows:

$$s^2 = \frac{\sum_{j=1}^{n}(c_j - \overline{c})^2}{n-1} \tag{11}$$

The mean value of the sensitive IMF variance can then be calculated as:

$$\Delta = \frac{\sum_{k=1}^{n} s^2}{i} \tag{12}$$

3. The Algorithms and Results

The ship underwater radiated noise signals will generate IMF components after EEMD decomposition, and each component represents the information of a sound source inside the ship, including the engine, propeller, various pipe mechanical vibrations, and other signals, as well as the sea state information at the time of signals acquisition. With the change of ship navigation conditions and sea state, each parameter in the signals will change, and no direct and separate relationship can be established between each parameter and the sound source, so it is necessary to select or establish more stable characteristic parameters for ship type identification.

From the 340 processed data, 20 samples are randomly selected for each type of underwater radiated noise, giving a total of 80 samples, and these samples are analyzed to explore the effective feature parameters for identifying ship types.

The traditional way of dividing the high frequency region and the low frequency region is referred to in the literature [29], where the frequency value between 100 Hz and 1000 Hz is defined as the low frequency region of ship-borne noise and 1000–10,000 Hz as the high frequency region in this study. The difference between the high frequency region and the low frequency region of the ship-radiated noise energy is defined as the difference between the high frequency and low frequency energy of the ship. Figure 4a shows the difference in high and low frequency energy obtained using the traditional method, and it can be seen that this method can classify ship noise into two categories, but a finer classification cannot be made. For example, passenger ship noise and tug noise cannot be distinguished, and tanker noise and tug noise cannot be distinguished.

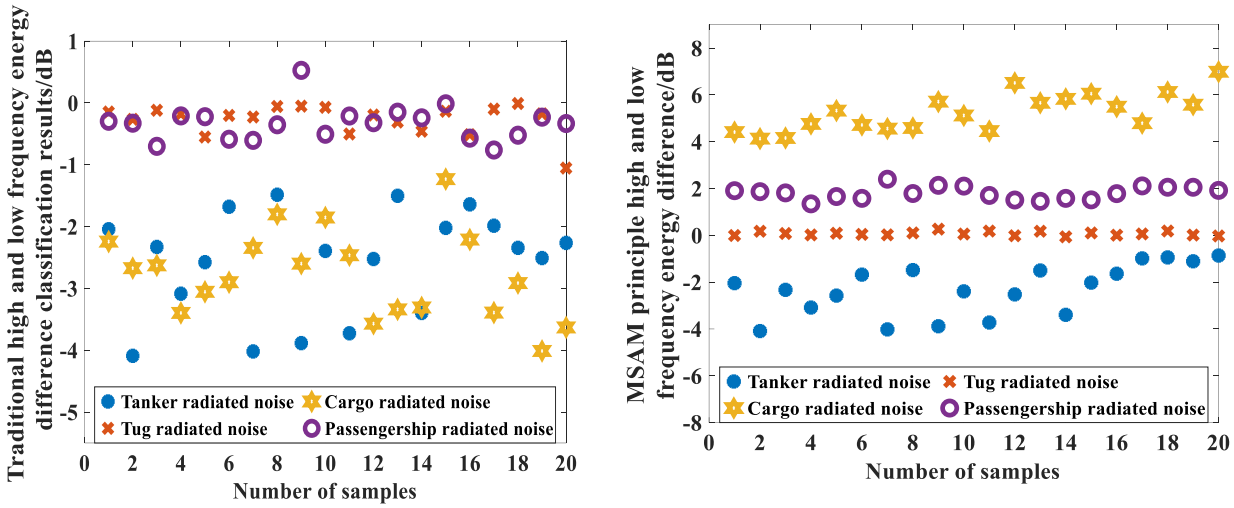

(a) (b)

Figure 4. (**a**) Classification results from the traditional method of high and low frequency energy difference; (**b**) Classification results from the self-adaptive method of high and low frequency energy difference.

The classification results of the adaptive high frequency and low frequency energy difference determined by the MSAM principle are shown in Figure 4b, and the high frequency and low frequency energy difference of various types of ship noise have type consistency, and the adaptive high frequency and low frequency energy difference can be used as a method of ship noise identification and classification.

Figure 4 shows the results of ship type differentiation by high and low frequency energy difference after adaptively dividing high frequency and low frequency based on the MSAM principle and using the deviation scale h_v as the judgment criterion. As can be seen from the figure, the high and low frequency energy differences of the same type of ship underwater radiated noise are not exactly equal but generally hover around a mean value. For different types of ship underwater radiated noise, the high and low frequency energy

differences have large differences and have good differentiability. Table 2 shows the range of high and low frequency energy differences based on the MSAM principle obtained on the basis of the selected 20 samples.

Table 2. Self-adaptive Range of High and Low Frequency Energy Difference based on MSAM Principle (20 samples).

Type	High and Low Frequency Energy Difference Range/dB	Type	High and Low Frequency Energy Difference Range/dB
Oil tanker underwater radiated noise	−4.0905~−0.8639	cargo vessel underwater radiated noise	4.1328~6.9894
tugboat underwater radiated noise	−0.0648~0.2654	Passenger ship underwater radiated noise	1.3457~2.3984

Figure 5 shows the mean value of the variance of the four types of underwater radiated noise samples obtained on the basis of the derived IMF sensitivity factor. It can be observed that the detection performance of tanker underwater radiated noise and cargo underwater radiated noise are the best, and the detection performance of tug noise and passenger ship underwater radiated noise are the second best, and the detection performance of this feature parameter is obviously different from that of the adaptive high and low frequency energy difference as a criterion. This parameter can be used as another feature value for ship classification. Table 3 shows the mean range of the sensitive IMF variance obtained from the selected 20 samples.

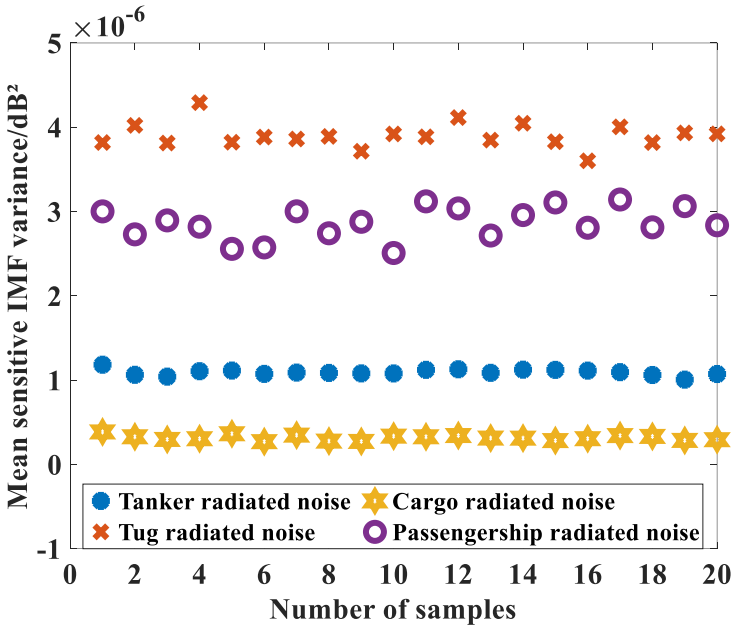

Figure 5. Mean sensitive IMF variance of the four types of ship underwater radiated noises.

Table 3. Mean Range of sensitive IMF variance (20 samples).

Type	Mean Range of Sensitive IMF Variance/dB^2	Type	Mean Range of Sensitive IMF Variance/dB^2
Oil tanker underwater radiated noise	1.0060×10^{-6}~1.1829×10^{-6}	Cargo vessel underwater radiated noise	2.7007×10^{-7}~3.8535×10^{-7}
Tugboat underwater radiated noise	3.8127×10^{-6}~4.2921×10^{-6}	Passenger ship underwater radiated noise	2.5572×10^{-6}~3.1428×10^{-6}

Identification Method of Ship Type Based on Bicharacteristic Parameters

From the above analysis, it can be seen that the degree of identification of different types of ship underwater radiated noise varies when the two methods are used separately to classify and identify ship underwater radiated noise, and now the two methods are combined with observing their effects.

Using the MSAM principle of adaptive high and low frequency energy difference and sensitive IMF variance mean dual feature parameters, 20 randomly selected underwater radiated noise samples are classified, as shown in Figure 6. It can be observed that passenger ship underwater radiated noise has the best data aggregation, while cargo underwater radiated noise, tanker underwater radiated noise, and tug underwater radiated noise are each distributed in a rectangular area.

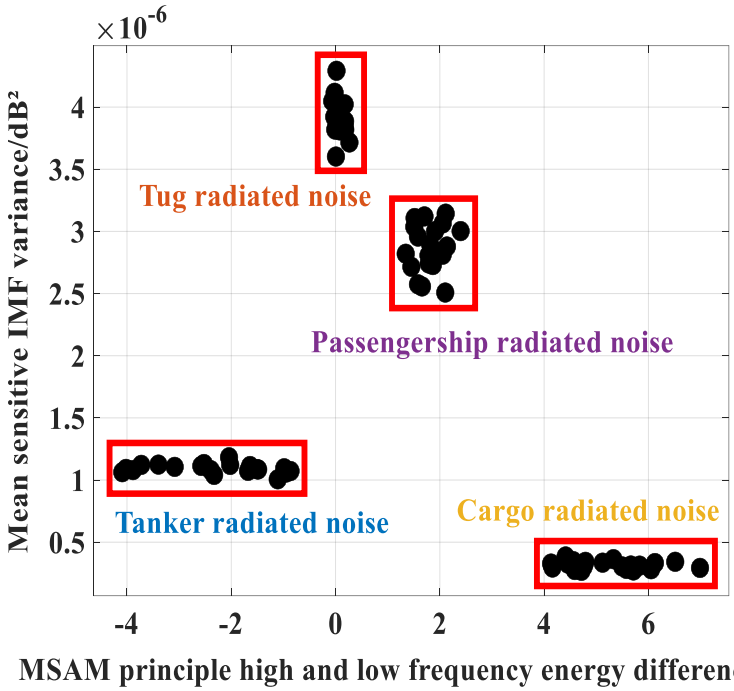

Figure 6. Distribution of bicharacteristic parameters of the ship underwater radiated noises.

4. Discussion

The ship type identification is based on two feature parameters, adaptive high and low frequency energy difference and sensitive IMF variance mean, and the filtered data are allocated in the ratio of 6:4 between the training set and the test set to verify the recognition rate of the dual feature parameters. The experiments show an accuracy of 96.25% with good recognition.

To further verify the applicability of the above two methods, validation experiments were conducted at Qingdao National Central Fishing Port. The fishing port is dominated by small and medium-sized fishing boats, and the main two main types of boats are named large fishing boats and small fishing boats. Eight fishing boats of each type were selected and analyzed, and the results are shown in Figure 7. The observation results show that as the same type of fishing vessels, regardless of the differences in models, their adaptive high and low frequency energy difference and sensitive IMF variance mean values are in a range, and when using the above two characteristic parameters for classification, it is possible to discriminate them as the same type of vessels.

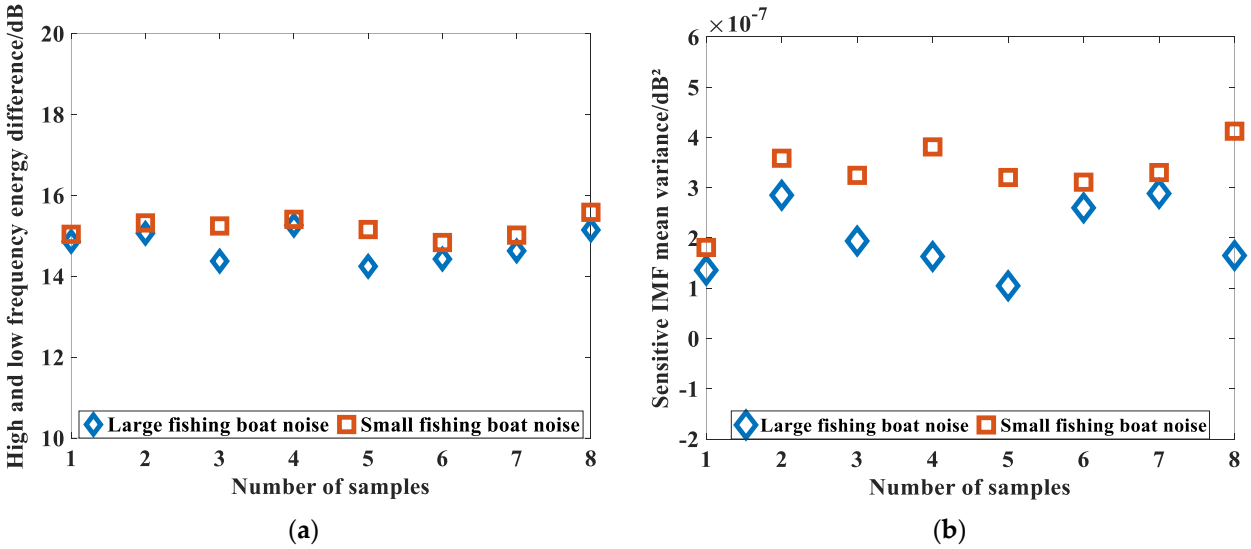

Figure 7. High and low frequency energy difference and sensitive IMF variance from fishing boats. (**a**) Self-adaptive high and low frequency energy difference; (**b**) sensitive IMF mean-variance.

All underwater radiated noise samples in the DeepShip dataset are obtained at the location where the hydrophone is closer to the ship, with a distance variation between 200 m and ~2000 m. In order to compare the changes in identification efficiency of two feature parameter types at different measurement distances, underwater radiated noise data obtained at four distance classes of 300 m, 1000 m, 1500 m, and 2000 m were selected, and a representative sample of each type of ship is selected and subjected to adaptive noise reduction and un-noise reduction respectively.

The results of the identification of the two feature parameter types, adaptive high and low frequency energy difference and sensitive IMF variance, at four different distances, are shown in Figure 8. Where Figure 8a,c uses unfiltered ship underwater radiated noise and Figure 8b,d uses filtered ship underwater radiated noise. Comparing Figure 8a,b and Figure 8c,d, it can be seen that the filtered underwater radiated noise is best identified at a close distance of 300 m, and as the distance increases, the high and low frequency energy difference and the mean value of the sensitive IMF variance of each type of underwater radiated noise have different changes, but the four types of ship underwater radiated noise can still be identified; The unfiltered underwater radiated noise can also be well discriminated at a distance of 300 m, but as the distance increases, the relative difference between the different types of underwater radiated noise becomes smaller and smaller, and the discriminability becomes less and less. This is because as the distance increases, other factors, such as the background underwater radiated noise of the marine environment and the reflection of the seabed medium, become more influential, making the components in the underwater radiated noise signal more complex.

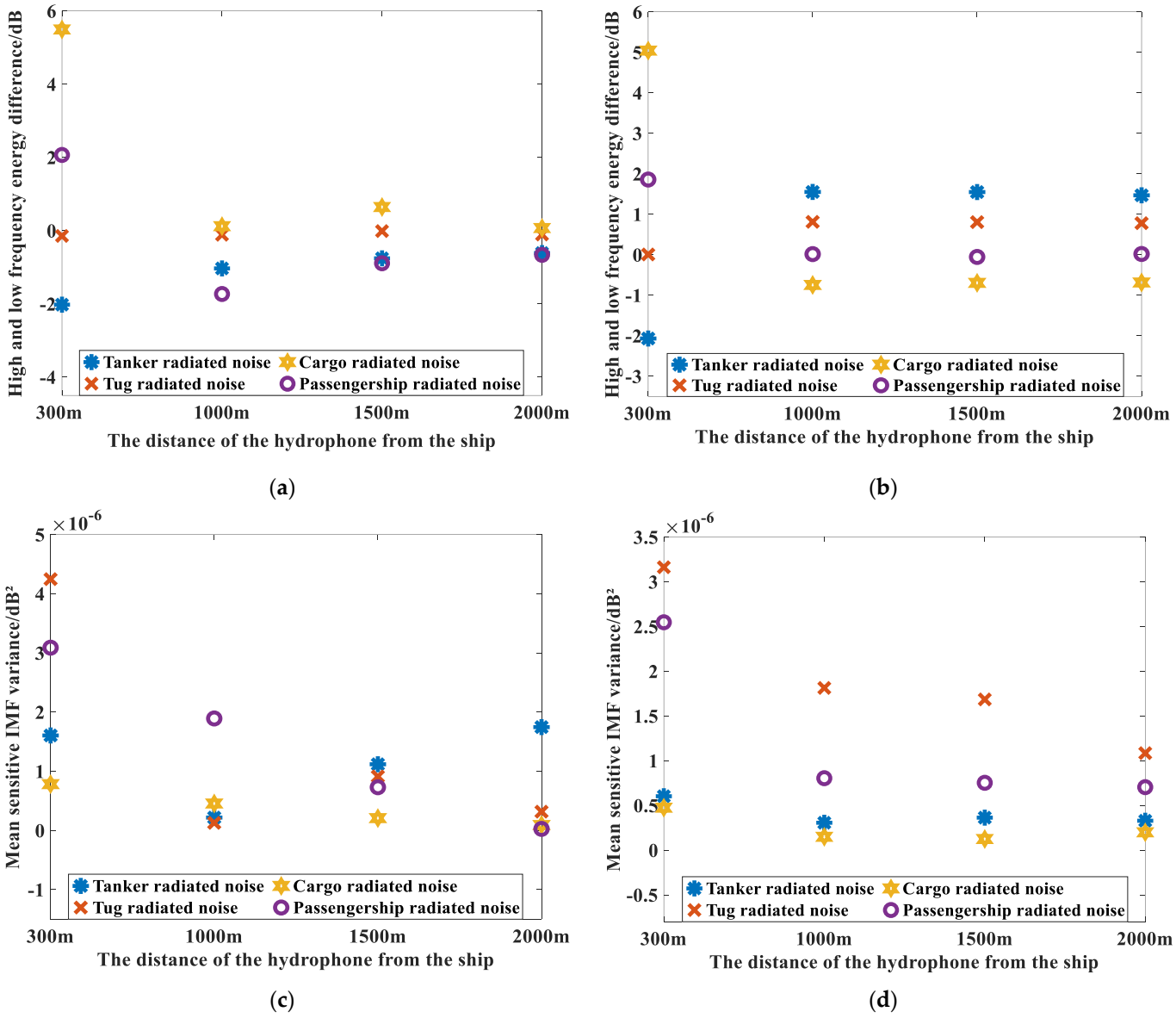

Figure 8. High and low frequency energy difference and sensitive IMF variance of unfiltered and filtered ship underwater radiated noises at different distances. (**a**) Differential high and low frequency energy of radiated noise from uncancelled vessels; (**b**) Differential high and low frequency energy of radiated noise from noise-reduced vessels; (**c**) Mean value of the variance of the radiation noise sensitive IMF for unabated ships; (**d**) Noise-reduced ship radiation noise sensitive IMF variance mean.

To further determine the ability to identify ship types at different distances, 20 samples are selected for each type of ship underwater radiated noise at each of the above four distances, giving a total of 320 samples. The identification was first performed with the adaptive high and low frequency energy difference, then the sensitive IMF variance mean was added, and the identification results are shown in Table 4.

Table 4. Improvement of bicharacteristic parameters on ship type distance identification rate.

Type	Distance	Identification Rate of Self-Adaptive High and Low Frequency Energy Difference	Identification Rate with Sensitive IMF Variance Mean Added to the Left Column
Oil tanker underwater radiated noise	300 m	90%	95%
	1000 m	60%	70%
	1500 m	60%	70%
	2000 m	60%	70%
Cargo vessel underwater radiated noise	300 m	95%	100%
	1000 m	70%	75%
	1500 m	70%	75%
	2000 m	70%	75%
Tugboat underwater radiated noise	300 m	85%	95%
	1000 m	60%	75%
	1500 m	60%	75%
	2000 m	60%	75%
Passenger ship underwater radiated noise	300 m	100%	100%
	1000 m	75%	80%
	1500 m	75%	80%
	2000 m	75%	80%

Observing Table 4, it can be seen that when using the adaptive high frequency and low frequency energy difference parameters are used for identification, the identification rate is best at 300 m, and the identification effect becomes weaker and does not change much at 1000~2000 m; when the sensitive IMF variance mean parameter is added, the type resolution is improved at all distances. Thus, it can be proved that the identification of four types of ship types in this dataset is effective in the range of 2000 m using the dual feature parameter method.

In the above study, it is the identification of ship types using underwater radiated noise, including cargos, passenger ships, tankers, and tugs. This paper tries to identify the individuals of ships, and it is found that passenger ships have the worst identifiability, tugs are the second, and cargos and passenger ships are the best. This is because the classification aggregation of passenger ships is the best, which leads to the most complicated identification of their individuals, and the individual differences between cargo and passenger ships are large, and the identification is relatively simple. This also gives some indication of the direction of the next step of individual identification.

5. Conclusions

This paper illustrates the importance of ship classification and identification in environmental protection, shipping management, and security and defense. Firstly, the limitations of the traditional time-frequency domain analysis method in the study of ship noise underwater radiated noise analysis are analyzed, and then the feature extraction of ship noise underwater radiated noise based on EEMD with dual feature parameters is proposed.

The article improves on the traditional high and low frequency energy difference by introducing the MSAM principle into the field of noise underwater radiation noise classification and identification, transforming the division of high and low frequency order energy from a fixed method to an adaptive method, which improves the accuracy of high and low frequency energy difference classification. At the same time, the method of sensitive IMF variance averaging is introduced to focus attention on the sensitive IMF and its preceding higher-order modal components. Finally, the combination of the above

two characteristic parameters is used as the basis for determining the type identification of four types of ship noise underwater radiated noise. After the type identification method was established, the repeatability and applicability of the method were extended using measured underwater radiated noise data from fishing vessels; the recognition rates of ship noise underwater radiated noise classifications at different distances were compared, and it was found that factors such as marine environmental noise underwater radiated noise and seafloor reflections constrained the recognition distances.

The maximum distance of this dataset is 2 km, which is sufficient for environmental protection and port planning; for the problem of classification and identification of radiation noise from ships, the main objective of this paper is to propose a feature extraction method, verify the accuracy of the relevant method, and in the future the method can be combined with neural networks and other contents, which can easily and conveniently achieve type identification, or even ship class identification or individual identification under the same type.

The method has some limitations, such as how to ensure the effectiveness of the identification method when there are enough ship types or when the ship types and models are too similar. Therefore, future development can be explored from the following perspectives: (1) expand the data source and explore the feasibility and practicality in a larger database; (2) continue to identify the type of ships or individual identification from different perspectives, for example, it can start from the direction of tonnage, speed, engine model, etc.

Author Contributions: Conceptualization, S.C. and S.G.; methodology, S.C. and S.G.; software, S.C.; data curation, H.W. and N.Y.; writing-original draft preparation, S.C. and S.G.; writing-review and editing, S.G. and Z.W.; supervision Z.W.; project administration, S.C. All authors have read and agreed to the published version of the manuscript.

Funding: The National Key Research and Development Program of China (Grant No. 2021YFC3101100). The Marine S&T Fund of Shandong Province for Pilot National Laboratory for Marine Science and Technology (Qingdao) (No. 2018SDKJ0101-2).

Institutional Review Board Statement: Not applicable.

Informed Consent Statement: Not applicable.

Data Availability Statement: Restrictions apply to the availability of these data. Data was obtained from IRFAN M et al., and are available from the authors with the permission of IRFAN M et al.

Acknowledgments: The dataset used in this study (the Deepship dataset) was provided by IRFAN M et al., for which we would like to express our heartfelt thanks.

Conflicts of Interest: The authors declare no conflict of interest.

References

1. Li, Q. Advances of research work in underwater acoustics. *Acta Acust.* **2001**, *26*, 295–301.
2. Hong, F.; Liu, C.; Guo, L.; Chen, F.; Feng, H. Underwater acoustic target recognition with a residual network and the optimized feature extraction method. *Appl. Sci.* **2021**, *11*, 1442. [CrossRef]
3. Xie, D.; Sun, H.; Qi, J. A new feature extraction method based on improved variational mode decomposition, normalized maximal information coefficient and permutation entropy for ship-radiated noise. *Entropy* **2020**, *22*, 620. [CrossRef] [PubMed]
4. Licitra, G.; Bolognese, M.; Palazzuoli, D.; Fredianelli, L.; Fidecaro, F. Port Noise Impact and Citizens' Complaints Evaluation in RUMBLE and MON ACUMEN INTERREG Projects. In Proceedings of the 26th International Congress on Sound and Vibration, Montreal, QC, Canada, 7–11 July 2019; pp. 7–11.
5. Murphy, E.; King, E.A. An assessment of residential exposure to environmental noise at a shipping port. *Environ. Int.* **2014**, *63*, 207–215. [CrossRef]
6. Fredianelli, L.; Nastasi, M.; Bernardini, M.; Fidecaro, F.; Licitra, G. Pass-by characterization of noise emitted by different categories of seagoing ships in ports. *Sustainability* **2020**, *12*, 1740. [CrossRef]
7. Nastasi, M.; Fredianelli, L.; Bernardini, M.; Teti, L.; Fidecaro, F.; Licitra, G. Parameters affecting noise emitted by ships moving in port areas. *Sustainability* **2020**, *12*, 8742. [CrossRef]
8. Schiavoni, S.; D'Alessandro, F.; Borelli, D.; Fredianelli, L.; Gaggero, T.; Schenone, C.; Baldinelli, G. Airborne Sound Power Levels and Spectra of Noise Sources in Port Areas. *Int. J. Environ. Res. Public Health* **2022**, *19*, 10996. [CrossRef]

9. Fredianelli, L.; Gaggero, T.; Bolognese, M.; Borelli, D.; Fidecaro, F.; Schenone, C.; Licitra, G. Source characterization guidelines for noise mapping of port areas. *Heliyon* **2022**, *8*, e09021. [CrossRef]
10. Fredianelli, L.; Bolognese, M.; Fidecaro, F.; Licitra, G. Classification of noise sources for port area noise mapping. *Environments* **2021**, *8*, 12. [CrossRef]
11. Li, Z.; Li, Y.; Zhang, K. A feature extraction method of ship-radiated noise based on fluctuation-based dispersion entropy and intrinsic time-scale decomposition. *Entropy* **2019**, *21*, 693. [CrossRef]
12. Liu, Z.; Cui, Y.; Li, W. A classification method for complex power quality disturbances using EEMD and rank wavelet SVM. *IEEE Trans. Smart Grid* **2015**, *6*, 1678–1685. [CrossRef]
13. Ioana, C.; Quinquis, A.; Stephan, Y. Feature extraction from underwater signals using time-frequency warping operators. *IEEE J. Ocean. Eng.* **2006**, *31*, 628–645. [CrossRef]
14. Huynh, Q.Q.; Cooper, L.N.; Intrator, N.; Shouval, H. Classification of underwater mammals using feature extraction based on time-frequency analysis and BCM theory. *IEEE Trans. Signal Process.* **1998**, *46*, 1202–1207. [CrossRef]
15. Gabor, D. Theory of communication. Part 1: The analysis of information. *J. Inst. Electr. Eng.-Part III Radio Commun. Eng.* **1946**, *93*, 429–441. [CrossRef]
16. Esmaiel, H.; Xie, D.; Qasem, Z.A.; Sun, H.; Qi, J.; Wang, J. Multi-stage feature extraction and classification for ship-radiated noise. *Sensors* **2022**, *22*, 112. [CrossRef] [PubMed]
17. Cohen, I.; Raz, S.; Malah, D. Orthonormal shift-invariant wavelet packet decomposition and representation. *Signal Process.* **1997**, *57*, 251–270. [CrossRef]
18. Dasgupta, N.; Runkle, P.; Couchman, L.; Carin, L. Dual hidden Markov model for characterizing wavelet coefficients from multi-aspect scattering data. *Signal Process.* **2001**, *81*, 1303–1316. [CrossRef]
19. Tucker, S.; Brown, G.J. Classification of transient sonar sounds using perceptually motivated features. *IEEE J. Ocean. Eng.* **2005**, *30*, 588–600. [CrossRef]
20. Azimi-Sadjadi, M.R.; Yao, D.; Huang, Q.; Dobeck, G.J. Underwater target classification using wavelet packets and neural networks. *IEEE Trans. Neural Netw.* **2000**, *11*, 784–794. [CrossRef]
21. Runkle, P.; Carin, L.; Couchman, L.; Bucaro, J.A.; Yoder, T.J. Multiaspect identification of submerged elastic targets via wave-based matching pursuits and hidden Markov models. *J. Acoust. Soc. Am.* **1999**, *106*, 605–616. [CrossRef]
22. Bentley, P.M.; McDonnell, J. Wavelet transforms: An introduction. *Electron. Commun. Eng. J.* **1994**, *6*, 175–186. [CrossRef]
23. Huang, N.E.; Shen, Z.; Long, S.R.; Wu, M.C.; Shih, H.H.; Zheng, Q.; Yen, N.-C.; Tung, C.C.; Liu, H.H. The empirical mode decomposition and the Hilbert spectrum for nonlinear and non-stationary time series analysis. *Proc. R. Soc. London. Ser. A Math. Phys. Eng. Sci.* **1998**, *454*, 903–995. [CrossRef]
24. Wu, Z.; Huang, N.E. Ensemble empirical mode decomposition: A noise-assisted data analysis method. *Adv. Adapt. Data Anal.* **2009**, *1*, 1–41. [CrossRef]
25. Li, Y.; Gao, P.; Tang, B.; Yi, Y.; Zhang, J. Double feature extraction method of ship-radiated noise signal based on slope entropy and permutation entropy. *Entropy* **2022**, *24*, 22. [CrossRef]
26. Yang, H.; Zhao, K.; Li, G. A new ship-radiated noise feature extraction technique based on variational mode decomposition and fluctuation-based dispersion entropy. *Entropy* **2019**, *21*, 235. [CrossRef] [PubMed]
27. Li, Y.; Tang, B.; Jiao, S. Optimized ship-radiated noise feature extraction approaches based on CEEMDAN and slope entropy. *Entropy* **2022**, *24*, 1265. [CrossRef] [PubMed]
28. Irfan, M.; Jiangbin, Z.; Ali, S.; Iqbal, M.; Masood, Z.; Hamid, U. DeepShip: An underwater acoustic benchmark dataset and a separable convolution based autoencoder for classification. *Expert Syst. Appl.* **2021**, *183*, 115270. [CrossRef]
29. Djurović, I.; Sejdić, E.; Jiang, J. Frequency-based window width optimization for S-transform. *AEU-Int. J. Electron. Commun.* **2008**, *62*, 245–250. [CrossRef]